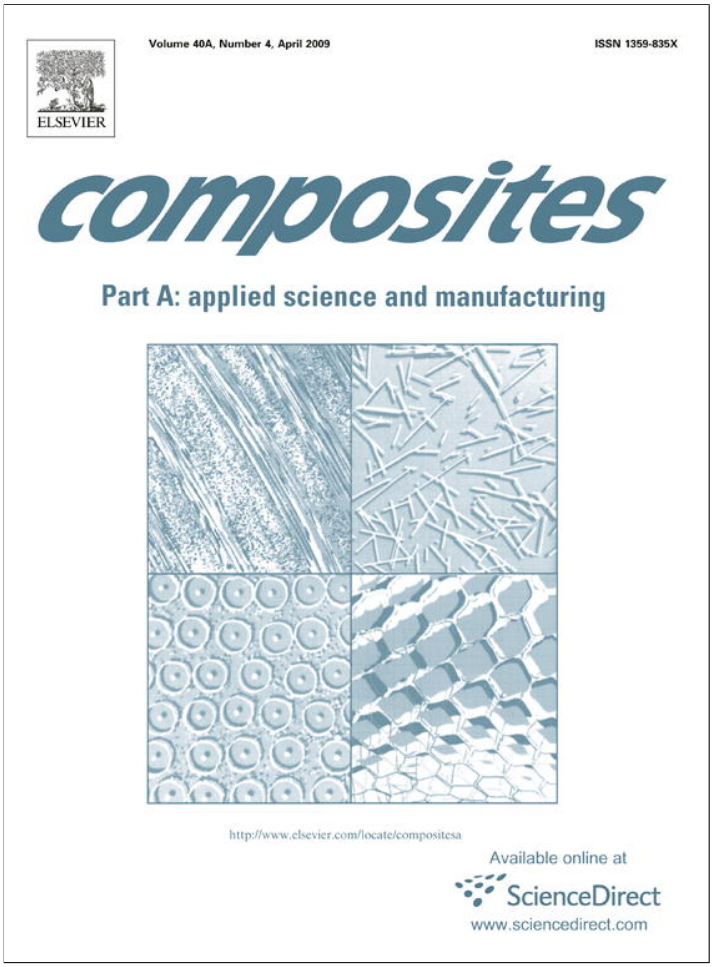

Composites: Part A 40 (2009) 388–393

Contents lists available at ScienceDirect

Composites: Part A

journal homepage: www.elsevier.com/locate/compositesa

Dielectric and magnetic response of Fe_3O_4/epoxy composites

L.A. Ramajo *, A.A. Cristóbal, P.M. Botta, J.M. Porto López, M.M. Reboredo, M.S. Castro

Institute of Research in Materials Science and Technology (INTEMA), CONICET – University of Mar del Plata, Juan B Justo 4302, B7608FDQ Mar del Plata, Argentina

ARTICLE INFO

Article history:
Received 12 September 2008
Received in revised form 21 December 2008
Accepted 22 December 2008

Keywords:
A. Polymer-matrix composites (PMCs)
B. Electrical properties
C. Magnetic properties

ABSTRACT

Magnetic and dielectric properties of Fe_3O_4/epoxy resin composites were studied as a function of Fe_3O_4 concentration. The Fe_3O_4 powder was milled using a planetary ball-mill in order to reduce the particle size. B.E.T. area of these particles was determined, and a structural characterization was performed by X-ray diffraction (XRD). Fe_3O_4/epoxy composites were prepared mixing the raw materials and pouring them into suitable moulds. Dielectric measurements were performed at different frequencies and temperatures, while magnetic properties were assessed at different temperatures. It was found that permittivity was strongly dependent on the filler concentration and frequency. Maxwell–Wagner–Sillars interfacial polarization, Intermediate Dipolar Polarization (IDE), and α relaxation process were responsible for the observed behavior. Magnetic measurements revealed the presence of magnetite nanoparticles in the composites, with a blocking temperature close to 170 K.

1. Introduction

There is a growing demand for multifunctional composites to meet special requirements of electronic components [1–2]. This can be achieved by the use of suitable fillers such as aluminum [3], carbon fibers and graphite [4], aluminum nitrides [5], nickel or silver particles [6], or barium titanate [7]. Furthermore, the magnetic properties of the polymer can be simultaneously improved by using a suitable particulate material.

Due to its good magnetic and electrical properties, magnetite (Fe_3O_4) is one of the preferred and best characterised filler materials, which is combined with polymers, i.e., to record media [8] and in medical applications [9]. Additionally, magnetite is used for magnetic products in the building industry for the absorption of hard- and X-radiation [10] or as microwave absorbers (electromagnetic shielding) in military or civil products [11]. The properties of Fe_3O_4 are unique because it is an oxide with a very high saturation magnetisation (92–100 emu/g) and an unusually low bulk resistivity ($1.068 \times 10^{-2}\ \Omega$cm) [12]. Therefore, magnetite has the potential for providing the desired magnetic and electrical properties to the final composite.

Excellent features of the ferrite/polymer composites make them quite attractive for applications not only as inductive and capacitive materials but also as microwave absorber materials. These characteristics are related to a sharply reduced dielectric loss compared to that of bulk ferrites, while microwave absorption properties remain uninfluenced owing to the domination of natural ferromagnetic resonance absorption [13]. In contrast to the frequency-limited application of the spinel type ferrites due to the Snoek's limit, hexagonal ferrites with high cut-off frequency in gigahertz (GHz) range are widely used as microwave absorber materials [14–16].

On the other hand, epoxy resins are excellent electrical insulators and protect electrical components from short circuiting, dust, and moisture. In the electronics industry, epoxy resins are the primary resin used in overmolding integrated circuits, transistors, and hybrid circuits, and in making printed circuit boards. Additionally, flexible epoxy resins are used for potting transformers and inductors.

In this work, polymer-based composites consisting of Fe_3O_4 fillers and epoxy resin were studied. These composites were made using pure epoxy and epoxy diluted in a solvent for reducing the polymer viscosity. The influence of filler concentration was studied by means of impedance spectroscopy. Electrical measurements were performed as a function of frequency and temperature in order to understand the relaxation processes. Also dc magnetisation was determined as a function of magnetic field and temperature in order to characterise the magnetic response of the composite.

2. Experimental

Epoxy D.E.R. 325 and curing agent D.E.H. 324, both of Dow Chemical, were chosen because of their good mechanical and dielectric properties [17–18]. So, following the manufacturer's recommendations, DEH 24 was mixed with the resin in a blend ratio of 12.5 phr [17]. Tetrahydrofuran (THF, Dorwil) was added to reduce the resin viscosity.

The magnetite was a concentrate of magnetite ore, from Sierra Grande (Rio Negro, Argentina), with $\geqslant$97.5 wt% Fe_3O_4. The major

* Corresponding author. Tel.: +54 223 481 6600; fax: +54 223 481 0046.
E-mail address: lramajo@fi.mdp.edu.ar (L.A. Ramajo).

1359-835X/$ - see front matter © 2009 Elsevier Ltd. All rights reserved.
doi:10.1016/j.compositesa.2008.12.017

impurities in magnetite were a clay mineral (illite) and quartz (both in similar concentrations). The powder was milled during 180 min using a planetary laboratory ball-mill (Fritsch, Pulverisette 7) with balls of hardened Cr-steel under Ar atmosphere (Po_2 <1 Pa). The milling bowls were loaded with 5 g of powder and 7 balls of 15 mm diameter each, resulting in a ball-to-powder mass ratio of 20:1. A rotation speed of 1500 rpm was used. This step reduced the particle size, which is necessary to achieve a good dispersion in the mixing process with the epoxy resin.

B.E.T. surface area of particles was determined using a Micromeritics FlowSorb II 2300, and lattice parameters were measured by X-ray diffraction using a XRD Philips PW 1830/40. TEM (Transmission Electron Microscopy) and SEM (Scanning Electron Microscopy) analyses, were performed using a Philips CM12 with an acceleration voltage of 100 kV and a JEOL 6460LV, respectively.

The ceramic powders were added to the epoxy resin at different volume fractions (from 10 to 40 volume fraction) and then, they were suitably blended for 5 min using an ultrasonic mixer (Sonic Vibra-Cell 150W). Before that, epoxy viscosity had been reduced using 10 wt% of THF. Each mixture was poured into glass moulds and cured at 100 °C for 2 h. Density was measured by Archimedes' method and theoretical density (ρ_T) was calculated using Eq. (1).

$$\rho_T = (1 - V) \cdot \rho_m + V \cdot \rho_p \quad (1)$$

where ρ_p is the filler density (5.2 g/cm^3), ρ_m is the matrix density (1.14 g/cm^3), and V is the volume fraction of filler.

Finally, samples were painted with silver paste and dielectric measurements were performed using a Hewlett Packard 4284A LCR meter from 20 Hz to 1 MHz and from 300 to 393 K.

Magnetisation loops as a function of magnetic field were measured at room temperature using a superconducting quantum interference device (SQUID), and a maximum field of 20 kOe. Moreover, magnetisation as a function of temperature at a constant magnetic field of 100 Oe was measured under a zero-field cooling (ZFC) regime.

3. Results and discussion

3.1. Magnetite characterisation

Fig. 1 shows the XRD spectra of milled and unmilled magnetite. Both samples presented the same diffraction peaks, although a decrease of the diffracted intensities, together with a marked broadening, was observed in milled magnetite due to their lower crystallinity and crystallite size, respectively [19]. B.E.T. surface areas of magnetite before and after milling were 0.6 and 3.0 m^2/g, respectively.

SEM micrographs of powders before and after milling are shown in Fig. 2. Both samples presented particle agglomeration, non-homogeneous distribution, and irregular particle shape. However, milled particles showed a smaller size in agreement with B.E.T. surface area results. The average particle size determined by image processing and analysis software, of particles before and after milling was 2.3 ± 1.3 μm (D_{max} = 11.21 μm and D_{min} = 0.13 μm) and 6.8 ± 3.7 μm (D_{max} = 16.25 μm and D_{min} = 1.53 μm), respectively. As it can be seen, even though the average values were different, the particle distribution was broad in both cases, and the maximum and minimum values were close for milled and non-milled particles.

3.2. Composites characterisation

The Fe_3O_4 volume fractions, obtained by TGA, and density for composites are shown in Table 1. The higher the filler concentration is, the more the density increases. The difference between experimental and theoretical density values was noticeable when the filler concentration increased. This behaviour was mainly due to the presence of small pores produced during the mixing process when air liberation was restricted due to the high viscosity of the system. However, differences between both, experimental and theoretical densities were lower than 6%, thus it can be neglected.

SEM micrographs of composites with different filler amount are shown in Fig. 3. Macro-pores were not found in any of the compos-

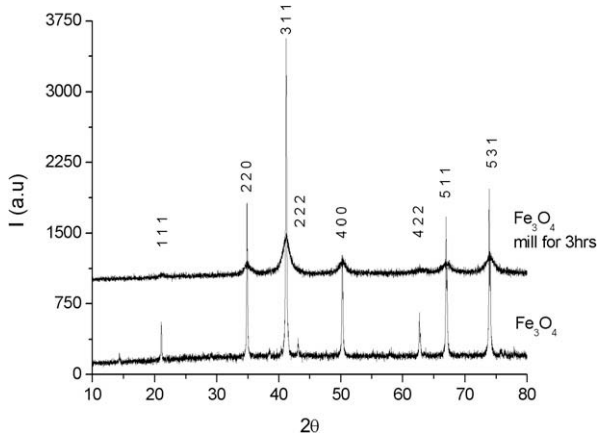

Fig. 1. XRD of magnetite before and after milling for 3 h.

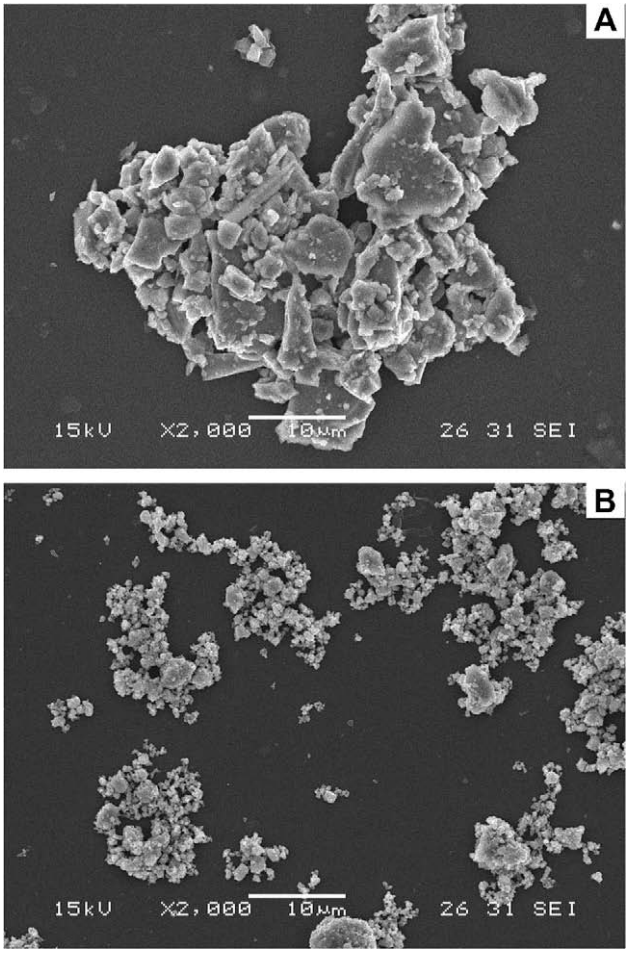

Fig. 2. SEM micrographs of magnetite before (A) and after (B) milling for 3 h.

Table 1
Theoretical and experimental density of composites with different filler concentrations.

Fe_3O_4 (vol%)	Theoretical density (g/cm^3)	Experimental density (g/cm^3)
11.4	1.59	1.57
20.1	1.94	1.93
30.1	2.35	2.24
40.5	2.77	2.59

ites, although all samples showed coarse particles and appreciable particle agglomeration as a consequence of the dry milling process (Fig. 2) and inefficient mixture step. Furthermore, systems with high particle concentration did not present a good contact between the particles and the resin (dark regions).

3.3. Dielectric properties

Room temperature real (ε') and imaginary (ε'') parts of permittivity for composites with different filler contents as a function of frequency are plotted in Fig. 4. It can be seen then, that the dielectric permittivity was strongly dependent on frequency and filler concentration. Higher values of ε' and ε'' were obtained at low frequencies because of the low resistivity of magnetite, which generated electric charge transference. In composites with higher volume fraction of particles (40% vol) a percolation effect appeared, increasing the electrical conductivity and dielectric loss. On the other hand, good dielectric properties, low loss tangent (closer to 0.06ε'), and relatively high dielectric constants (up to 30ε_0) were obtained at 1 kHz in systems with filler amount around 30 vol%.

In order to study the frequency and temperature dependence of relaxation processes, electrical modulus was analysed. Fig. 5 shows the real and imaginary parts of the electrical modulus [20] as a function of frequency at 393 K for all the composites. It can be seen that M' values increased with frequency and reached a rather constant value. A rise in the magnetite concentration produced a diminution in the M' in all the frequency range due to the higher real permittivity of the concentrated composites. Moreover, a peak in M'' curves can be observed, indicating a relaxation process which was not evident from the imaginary permittivity curves at the same temperature (393 K). These peaks corresponded to an α relaxation process and started to be evidenced at high temperatures, near the epoxy glass transition (T_g), as the mobility of polymer molecules was enhanced [21]. The maximum of M'' diminished for high filler's concentration, because the real permittivity ε' was increased.

The α relaxation peaks shifted at higher frequencies because of other relaxation processes. They can be influenced by two different effects. First, interfacial polarization effect, known as Maxwell–Wagner–Sillars (MWS), generated electric charge accumulation on the surface of the ceramic particles, displacing the relaxation peaks in heterogeneous systems [22]. Second, small particles, "nanoparticles", induced changes on the dynamics segmental relaxation of the polymer matrix due to changes in the local free volume and the inter- and intra-chain interactions. However, for micrometer-sized fillers, the enhanced polymer dynamics at the

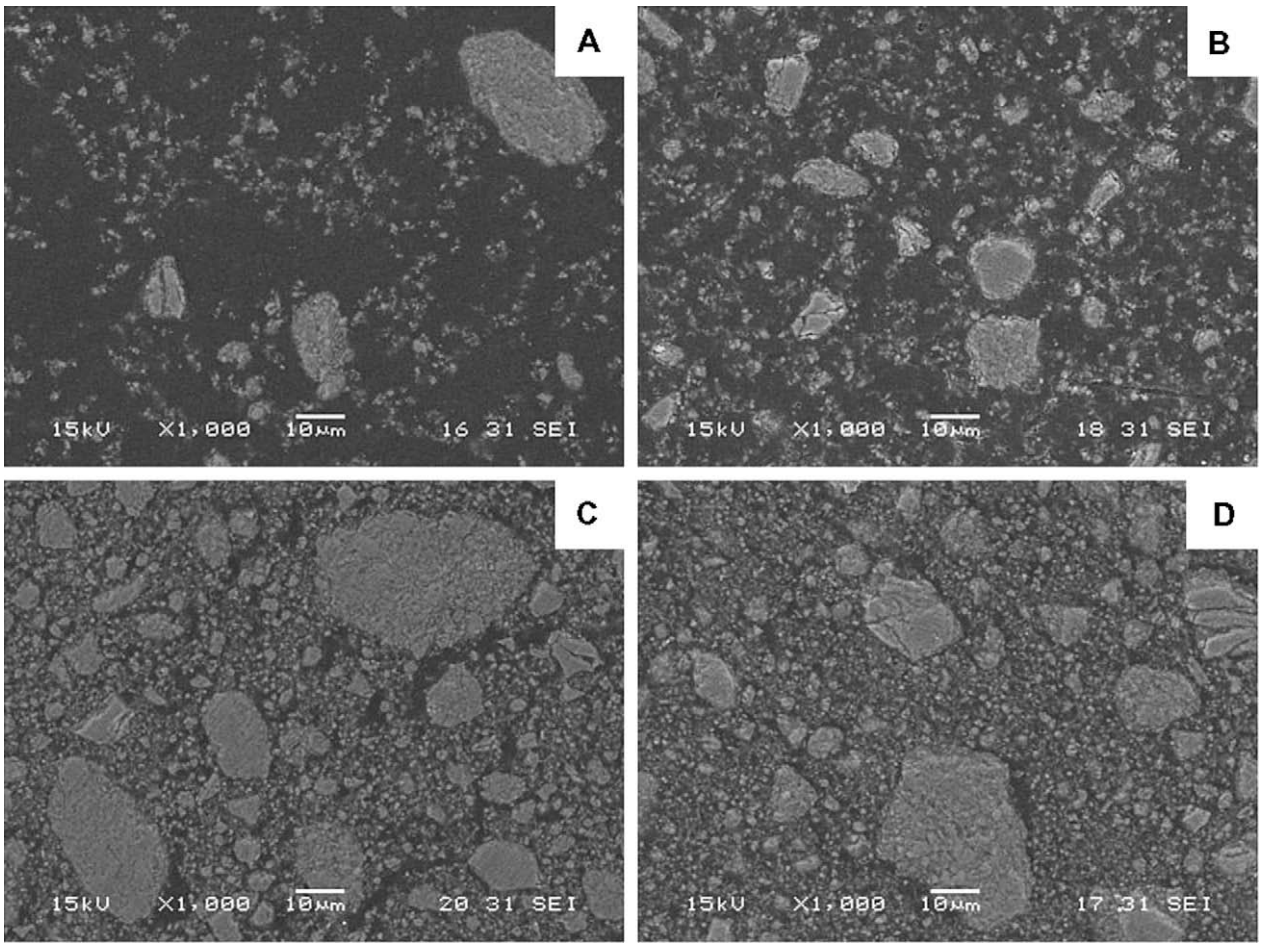

Fig. 3. SEM micrographs of composites with 10 (A), 20 (B), 30 (C), and 40 vol% (D). Bar 10 μm.

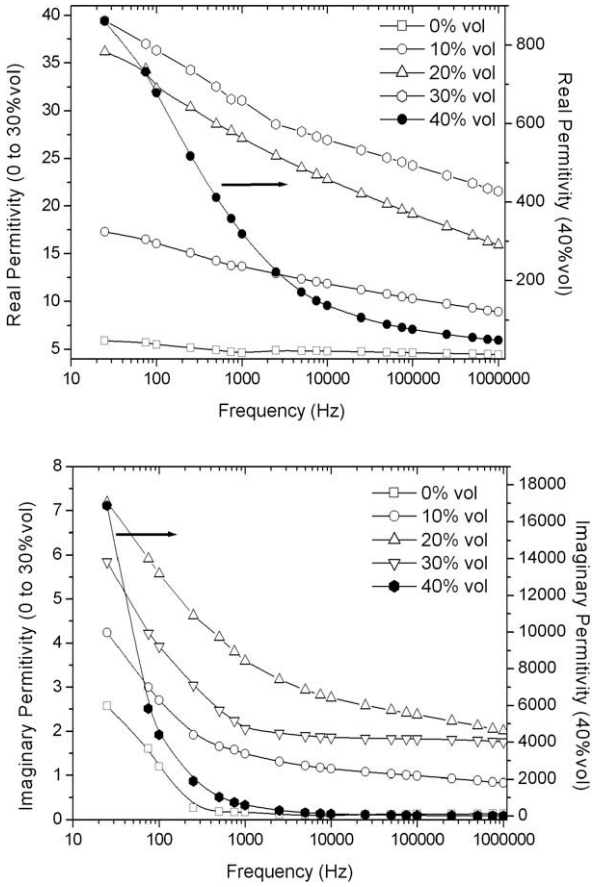

Fig. 4. Real (ε') and imaginary (ε'') permittivity vs. frequency curves of epoxy/Fe_3O_4 composites at 300 K.

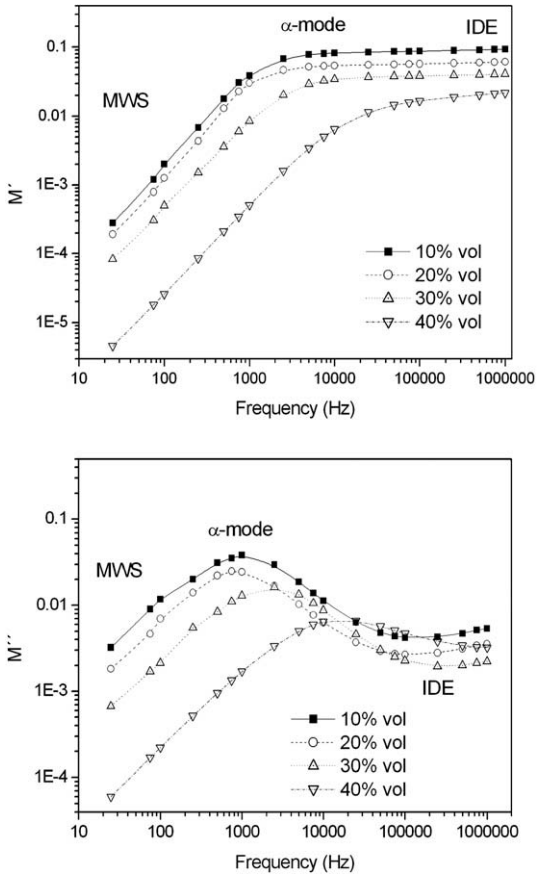

Fig. 5. Real (M') and imaginary (M'') electrical modulus vs. frequency at 393 K.

interface did not noticeably reduce or affect the relaxation frequency matrix because of the limiting interfacial area [23–25].

At extreme low and high frequencies interfacial polarization phenomena (MWS effects) and Intermediate Dipolar Effect mode (IDE-mode), respectively become evident. IDE-mode can be ascribed because of its appearance at high frequencies and its absence in the dielectric spectrum of the pure matrix [26]. So, the occurrence of this process is strongly affected by the filler's concentration and it is attributed to the ceramic material itself. Its location is intermediate in the dielectric spectra, lying between the fast (local modes) and the slow (α-mode and MWS effect) processes; thus it will be called Intermediate Dipolar Effect (IDE).

The combination of the three relaxation process (α-mode, MWS effect and IDE) was shown and fitted by Kontos et al. [26] on TiO_2-polymer. The IDE process became prevalent in those composites with high ceramic concentration. This fact implies that its origin should be sought in the polarization effects of the ceramic filler. In fact, Fe_3O_4 exhibited spontaneous polarization that might relax under the influence of an external alternating electric field [27].

The high temperature relaxation processes are also shown in the Cole–Cole representation (Fig. 6). Apart from the semicircle corresponding to α-mode, MWS relaxation could also be observed in the low frequency extreme. This fact was revealed by the asymmetry of the respective curves in the low frequency region where a hump was observed. The coincidence of the semicircles at early stages with the origin of the graph is a clear indication that no other relaxation process was present at lower frequencies in all studied composite systems. Moreover, the variation of the semicircle radius, corresponding to the α-mode, indicated that α-mode

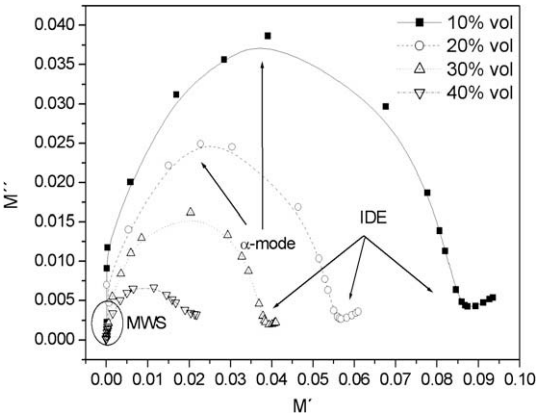

Fig. 6. Cole–Cole plots for all composite specimens at 393 K.

was influenced by the filler concentration [21]. Furthermore, at the high frequency end, experimental results from the composites with 10–40 vol% of Fe_3O_4 formed a suppressed semicircle reflecting the presence of Intermediate Dipolar Effect mode.

3.4. Magnetic properties

Fig. 7 shows the magnetic hysteresis loops obtained at room temperature for pure milled magnetite and the composites. For each sample, saturation magnetisation (M_s) and coercivity (H_c) values were taken from these curves. They are summarised in Table 2. This table also shows theoretical values of M_s which were calcu-

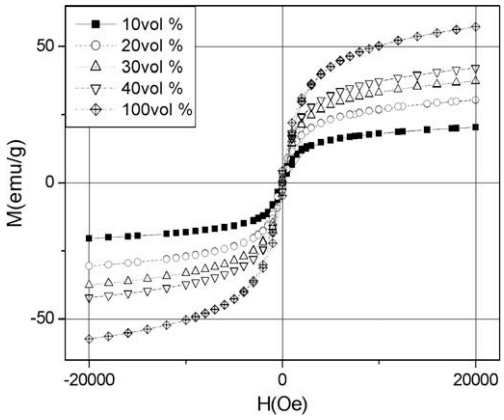

Fig. 7. Magnetic hysteresis loops for composites and milled Fe_3O_4 (at room temperature).

Table 2
Static magnetic properties of composites and milled Fe_3O_4 powder.

Fe_3O_4 (vol%)	Fe_3O_4 (wt%)	M_s (emu/g)	H_c (Oe)	Theoretical M_s (emu/g)
11.4	34.0	20.4	180	19.4
20.1	53.6	30.6	195	30.5
30.1	66.5	37.5	185	37.9
40.5	75.5	42.3	170	43.0
100	100	57.0	170	–

lated using the M_s measured for milled pure magnetite and the weight fraction of this oxide in each composite. An excellent agreement between calculated and measured M_s is observed for all the composites. This indicates that the method used for preparing the composite materials allows for accurately controlling the filler volume fraction and homogeneity.

It should be remarked that M_s of milled pure magnetite (57 emu/g) was considerably lower than that of unmilled magnetite (92 emu/g) [12], which was a consequence of the defect accumulation in the crystalline structure of magnetite during the prolonged ball-milling [27]. Also, the probable existence of nanometric particles could be another cause for this low M_s value.

A detailed inspection of the hysteresis loops revealed that they did not saturate at 15 kOe. This magnetic field was strong enough to achieve the saturation of magnetite, which is a very soft magnetic material. The absence of saturation even in pure magnetite indicates the presence of a paramagnetic phase in the inorganic filler. However, XRD patterns of milled magnetite did not reveal the presence of any impurity. A possible explanation for this fact is the formation of nanoparticles during the milling treatment of magnetite which could be in a superparamagnetic state at room temperature. In order to check this hypothesis, magnetisation measurements of milled magnetite as a function of temperature were performed (Fig. 8). A wide peak centred at about 170 K was observed in the ZFC curve, suggesting the blocking of the magnetite single-domain nanoparticles. Taking into account the large width of this peak, it was possible to conclude that the size distribution of the formed nanoparticles was really large. Furthermore, it is important to remark that the magnetisation curve had a significant contribution of micrometric multidomain particles. The inset in Fig. 8 shows a TEM image of milled magnetite revealing the existence of particles of 30–40 nm together with agglomerates of particles even smaller.

The presence of superparamagnetic nanoparticles in ball-milled magnetite was supported by a significant increase of coercivity measured at 100 K. A value of 490 Oe was obtained well below the blocking temperature while a coercivity of 170 Oe was measured at 300 K.

Coercivity values were nearly constant for all the samples, indicating that the coercive behavior was controlled by micrometer-sized particles, i.e., the typical particle-loading-independent coercivity response [28].

4. Conclusions

The dielectric and magnetic response of polymer composites consisting of an epoxy resin matrix and Fe_3O_4 magnetite ceramic

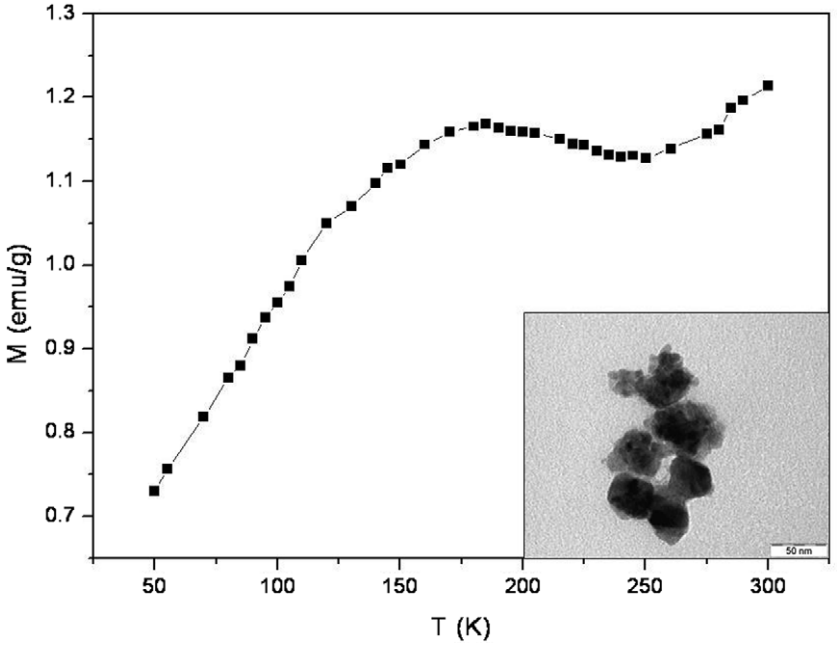

Fig. 8. Magnetisation (M) as a function of temperature at $H = 100$ Oe for milled magnetite. Inset: TEM micrograph revealing the presence of nanoparticles in the Fe_3O_4 powder.

filler have been studied in the frequency range of 20 Hz to 1 MHz and temperatures of 300 and 393 K. In this way, the following conclusions were drawn:

- Planetary ball-milling of magnetite produced a system with particle sizes ranged from nano to micrometer. This method was not efficient enough to produce a homogeneous particle distribution on composites microstructure. It could be improved using a wet process instead of the dry mill process employed.
- High permittivity and dielectric loss were obtained at low frequency in composites with 40 vol% of Fe_3O_4 because of magnetite percolation in the resin matrix. However, low loss was obtained in composites without percolation effect (lower than 40 vol%).
- Resin showed relaxation processes on all composites, while ceramic content influenced the real permittivity. Interfacial polarization processes known as Maxwell–Wagner–Sillars and Intermediate Dipolar Effect were generated by particles at low and high frequency, respectively. The first one produced an accumulation of charges on the interface that helped to displace peaks to higher frequencies while the latter increased M'' value at higher frequency.
- As expected, a continuous increment of saturation magnetisation with the magnetite weight fraction in the composites was observed. The coercivity followed the characteristic filler-loading independent response of soft magnetic microparticles.

Acknowledgements

This work was supported by the National Council of Science and Technology of Argentina (CONICET). It was also achieved thanks to material donation from Dow Chemical Argentina through the management of Ariadna Spinelli and Alfredo Fahnle. We owe gratitude to Prof. J. Rivas (University of Santiago de Compostela, Spain) for his invaluable help with magnetic measurements.

References

[1] Bai Y, Cheng Z-Y, Bharti V, Xu HS, Zhang QM. High-dielectric-constant ceramic-powder polymer composites. Appl Phys Lett 2000;25:3804–6.
[2] Kuo D-H, Chang C-C, Su T-Y, Wang WK, Lin B-Y. Behaviors of multi-doped $BaTiO_3$/epoxy composites. J Eur Ceram Soc 2001;21:1171–7.
[3] Wong CP, Bollampally RS. Thermal conductivity, elastic modulus, and coefficient of thermal expansion of polymer composites filled with ceramic particles for electronic packaging. J Appl Polym Sci 1999;74:3396–403.
[4] King JA, Tucker KW, Vogt BD, Weber EH, Quan C. Electrically and thermally conductive nylon 6,6. Polym Compos 1999;20:643–54.
[5] Xu Y, Chung DDL, Mroz C. Thermally conducting aluminum nitride polymer-matrix composites. Composites A 2001;32:1749–57.
[6] Göktürk HS, Fiske TJ, Kalyon DM. Effects of particle shape and size distributions on the electrical and magnetic properties of nickel/polyethylene composites. J Appl Polym Sci 1993;50:1891–901.
[7] Ramajo L, Reboredo MM, Castro MS. Characterization of epoxy/$BaTiO_3$ composites processed by dipping for integral capacitor films (ICF). J Mater Sci 2007;42:3685–91.
[8] Bate G. In: Wohlfahrt EP, editor. Ferromagnetic materials, vol. 2. Amsterdam: North-Holland; 1986. p. 381.
[9] Weidenfeller B, Höfer M, Schilling F. Thermal and electrical properties of magnetite filled polymers. Composites A 2002;33:1041–53.
[10] Cyrkiewicz M, Herling E, Klesczczewski J. Process for preparing ceramic-like materials and the ceramic-like materials. US Patent 5,683,616; 1997.
[11] Weidenfeller B, Riehemann W, Lei Q. Mechanical spectroscopy of polymer–magnetite composites. Mater Sci Eng A 2004;370:278–83.
[12] Liong S. A multifunctional approach to development, fabrication, and characterization of Fe_3O_4 composites. Doctoral Thesis, Georgia Institute of Technology; 2005.
[13] Ghasemi A, Hossienpour A, Morisako A, Saatchi A, Salehi M. Electromagnetic properties and microwave absorbing characteristics of doped barium hexaferrite. J Magn Magn Mater 2006;302:429–35.
[14] Li ZW, Lin GQ, Chen LF, Wu YP, Ong CK. Size effect on the static and dynamic magnetic properties of W-type barium ferrite composites: from microparticles to nanoparticles. J Appl Phys 2005;98:94310.
[15] Singh P, Babbar VK, Razdan A, Srivastava SL, Agrawal VK, Goel TC. Dielectric constant, magnetic permeability and microwave absorption studies of hot-pressed Ba-CoTi hexaferrite composites in X-band. J Mater Sci 2006;41:7190–6.
[16] Ruan S, Xu B, Suo H, Wu F, Xiang S, Zhao M. Microwave absorptive behavior of ZnCo-substituted W-type Ba hexaferrite nanocrystalline composite material. J Magn Magn Mater 2000;212:175–7.
[17] Dow liquid epoxy resins, selection guide, USA. Available from: http://www.dow.com.
[18] Ramajo L, Reboredo MM, Castro MS. Dielectric response and relaxation phenomena in composites of epoxy with $BaTiO_3$ particles. Composites A 2005;36:1267–74.
[19] Botta PM, Bercoff PG, Aglietti EF, Bertorello JM, Porto López HR. Synthesis and magnetic properties of zinc ferrite from mechanochemical and thermal treatments of Zn–Fe_3O_4 mixtures. Mater Sci Eng A 2003;360:146–52.
[20] Psarras GC, Manolakaki E, Tsangaris GM. Electrical relaxations in polymeric particulate composites of epoxy resin and metal particles. Composites A 2002;33:375–84.
[21] Psarras GC. Hopping conductivity in polymer matrix–metal particles composites. Composites A 2006;37:1545–53.
[22] Ramajo L, Reboredo M, Castro M. Dielectric response and relaxation phenomena in composites of epoxy with $BaTiO_3$ particles. Composites A 2007;28:1852–9.
[23] Kalogeras IM, Stathopoulos A, Vassilikou-Dova A, Brostow W. Nanoscale confinement effects on the relaxation dynamics in networks of diglycidyl ether of bisphenol-A and low-molecular-weight poly(ethylene oxide). J Phys Chem B 2007;111:2774–82.
[24] Krishnamoorti R, Vaia RA. Polymer nanocomposites. J Polym Sci B 2007;45:3252–6.
[25] Sun Y, Zhang Z, Moon K-S, Wong CP. Glass transition and relaxation behavior of epoxy nanocomposites. J Polym Sci B 2004;42:3849–58.
[26] Kontos GA, Soulintzis AL, Karahaliou PK, Psarras C, Georga SN, Krontiras CA, Pisanias MN. Electrical relaxation dynamics in TiO_2–polymer matrix composites. Express Polym Lett 2007;12:781–9.
[27] Botta PM, Bercoff PG, Aglietti EF, Bertorello HR, Porto López JM. Magnetic and structural study of mechanochemical reactions in the Al-Fe_3O_4 system. J Mater Sci 2002;37:2563–8.
[28] Guo Z, Park S, Hahn T, Wei S, Moldovan M, Karki AB, Young DP. Magnetic and electromagnetic evaluation of the magnetic nanoparticle filled polyurethane nanocomposites. J Appl Phys 2007;101:09M511.